Thermal and Combustion Behaviors of Aluminum/ Manganese Dioxide/ Fluoroelastomer Terpolymer Nanothermite

Jiaxing Song[1], Fei Duan[2], JIALIN CHEN[3], Guannan Wang[4], Quanwei Tian[1], and Jingkai Feng[1]

[1]Xi'an Rare Metal Materials Research Institute Co., Ltd.
[2]Nanyang Technological University
[3]Institute of Defense Engineering, AMS, PLA
[4]Xi'an Aerospace Propulsion Institute

August 16, 2022

Abstract

Fluoroelastomer has received increasing attention for energetic materials application due to its high fluorine contents. Different contents of poly(VDF-ter-HFP- ter- TFE) terpolymer are added into Al/MnO2 nanothermite. The peak exothermic temperature of thermite reaction for Al/MnO2 system is about 554 oC with 1070 Jg-1 heat release. After adding terpolymer, it mainly exists in the gap among Al nanoparticles and MnO2 nanorods, and can react with Al and MnO2 at the range of 350 oC to 540 oC before the occurrence of thermite reaction. 10wt% terpolymer has relatively little effect on the thermite reaction, and for the samples with higher terpolymer content, more nanothermite components reacts with terpolymer at early stage. Ignition and combustion performance show terpolymer can reduce ignition energy threshold by up to 9.82% and increase combustion duration time at least several times. The potential reasons for above results are analyzed. This work can shed light on application of fluoroelastomer in energetic-materials.

Thermal and Combustion Behaviors of Aluminum/ Manganese Dioxide/ Fluoroelastomer Terpolymer Nanothermite

Jiaxing Song*[a,b], Fei Duan*[b], Jialin Chen[c], Guannan Wang[d], Quanwei Tian[a] and Jingkai Feng[a]

[a] Xi'an Rare Metal Materials Research Institute Co., Ltd., Xi'an, 710016, China

[b] School of Mechanical and Aerospace Engineering, Nanyang Technological University, 639789, Singapore

[c] Institute of Defense Engineering, AMS, PLA, Beijing, 100036, China

[d] Xi'an Aerospace Propulsion Institute, Xi'an, 710100, China.

Corresponding author: sjx1407@126.com (Jiaxing Song); feiduan@ntu.edu.sg (Fei Duan).

Abstract : Fluoroelastomer has received increasing attention for energetic materials application due to its high fluorine contents. Different contents of poly(VDF-ter-HFP- ter- TFE) terpolymer are added into Al/MnO_2 nanothermite. The peak exothermic temperature of thermite reaction for Al/MnO_2 system is about 554 °C with 1070 Jg^{-1} heat release. After adding terpolymer, it mainly exists in the gap among Al nanoparticles and MnO_2 nanorods, and can react with Al and MnO_2 at the range of 350 °C to 540°C before the occurrence of thermite reaction. 10wt% terpolymer has relatively little effect on the thermite reaction, and for the samples with higher terpolymer content, more nanothermite components reacts with terpolymer at early stage. Ignition and combustion performance show terpolymer can reduce ignition energy threshold

by up to 9.82% and increase combustion duration time at least several times. The potential reasons for above results are analyzed. This work can shed light on application of fluoroelastomer in energetic-materials.

Keywords : fluoroelastomer; nanothermite; thermal analysis; combustion behaviors

1. Introduction

Nanothermite has received extensive attention as energetic materials for its excellent thermal, combustion and reaction characteristics with applications in propellants, explosives and pyrotechnics [1-2]. Conventionally, nanothermite consists of two components, a fuel and an oxidizer [1-2]. Comprehensively considering the cost, calorific value and safety, aluminum (Al) nanoparticles is the most popular choice for the fuel[3]. As for oxidizer, there are so many potential candidates, such as copper oxide (CuO), iron oxide (Fe_2O_3), silicon dioxide (SiO_2), manganese dioxide (MnO_2), nickel oxide (NiO) [4-10]. Among them, the formula of Al and MnO_2 is one of the most promising energetic materials with a high burning rate, an adiabatic temperature and a relatively low ignition point [11]. In nature, fluorine is the most electronegative element in periodic table of elements with the electronegativeity of 3.98 on Pauling scale [12-13]. Thus, recently, the combination of nanothermites and fluorine polymers has aroused wide concern from researchers [14-16].

Fluorine polymers have been already widely used in many applications, such as membrane, tubing, fibers, filler and coating materials, which contain fluorine atoms in the molecular chains [17-19]. The most famous fluorine polymer is polytetrafluroethylene (PTFE) because of the highest fluorine content, about 76% [20]. Tang and his co-author had paid much attention on the mechanical properties and impact-induced characteristics of PTFE/Al/CuO reactive materials [21-22]. The flame and energy release rate greatly improved due to the addition of Al/CuO thermite. Recently, a comparative research reported about three kinds of PTFE-based thermite materials, PTFE/Al/Fe_2O_3, PTFE/Al/$MnO_2$and PTFE/Al/MoO_3 [23]. The results showed that the formula of PTFE/Al/MnO_2 released the most energy during compression, and the detailed thermal reaction processes of PTFE/Al/MnO_2 was also reported [24]. But the components were mainly at the micron-scale with slow energy release. In fact, because of the poor solubility and agglomeration of PTFE, it is hard to obtain the uniform well-mixed samples, especially for nanothermites, which is also the main drawback for further application in energetic materials field [25]. Thus, poly(vinylidene fluoride-ter-hexafluoropropylene-ter-tetrafluoroethylene) (poly(VDF- ter- HFP-ter - TFE)) terpolymer with both high fluorine content and good solubility can be used as a substitute for PTFE in nanoenergetic materials application [25]. However, few researches focus on the application of poly(VDF- ter- HFP-ter - TFE) on nanothermites.

Therefore, in this paper, poly(VDF- ter- HFP-ter - TFE) terpolymer is selected as energetic additive and binder, and the Al/MnO_2/ poly(VDF- ter- HFP-ter - TFE) nanothermite samples are prepared by using electrospray method. The morphologies, thermal properties and combustion performance are investigated. Furthermore, the mechanism of terpolymer on nanothermite system is also discussed and analyzed which will provide a practical guidance for fluorine- containing nanothermite research and application.

2. Experimental Section

2.1 Materials

All chemicals can be used directly without any further purification any more. Al nanoparticles (Al NPs) (˜100nm diameter) are purchased from Shanghai Nai-ou Nano Technology Co., LTD, and the thickness of alumina shell on the surface of Al NPs is about 5 nm, so the active aluminum content is about 64.5%. Potassium hypermanganate ($KMnO_4$) (>99.5%) and concentrated hydrochloric acid (HCl) (36.0%˜38.0%) are supplied by Shanghai Lingfeng Chemical Reagent Co., LTD for further MnO_2 synthesis. MnO_2 nanorods (MnO_2 NRs) are synthesized via hydrothermal method at 140 °C for 12 h, please see Ref.[26-27]. Poly(VDF-ter- HFP-ter - TFE) terpolymer is selected from Shanghai 3F New Chemical Materials Co., LTD, with about 67.5% fluorine content. As for solvents and dispersant, ethyl alcohol, deionized water and dimethylformamide (DMF) are purchased from Nanjing Chemical Reagent Co., LTD.

2.2 Sample Preparation

The ratio of each component is listed in Table 1. In a typical preparation experiment, the mixture of Al NPs and MnO_2 NRs is dispersed in ethyl alcohol by using ultrasonic method. In the meanwhile, the corresponding poly(VDF- ter- HFP-ter - TFE) terpolymer component is dissolved by DMF. Then, the terpolymer -DMF solution is poured into the mixture of Al NPs and MnO_2 NRs as the precursor for further electrospray method. The diagram of electrospray experiment is shown in Figure 1. The precursor is put into the syringe with a 0.43 mm flat nozzle. The distance between the end of nozzle and the receiving plate is about 10 cm, and there is a 14 kV DC voltage loaded onto the distance. The precursor is ejected by a syringe pump with the velocity of 4.0 mL h^{-1}. During the process, the solvent volatilized and solid-state samples attach to the receiving plate. Finally, the samples are gently scraped off from the receiving plate for further tests.

Table 1 The detailed ratio of each component

No.	Al NPs /mg	MnO_2 NRs /mg	P(VDF-HFP-TFE)/mg	Mass fraction of terpolymer /%
AMT-0	40	60	0	0
AMT-1	40	60	12	10
AMT-2	40	60	25	20
AMT-3	40	60	43	30

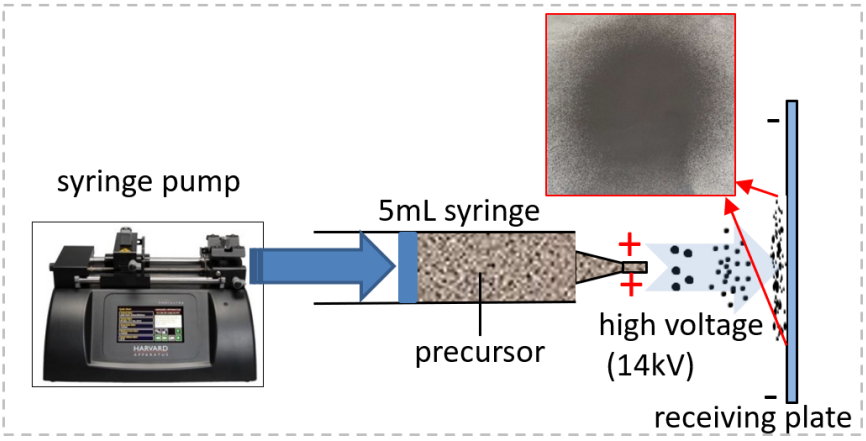

Figure 1 The diagram of electrospray experiment

2.3 Characteristics Analysis

The structures and morphologies of samples prepared from electrospray method are observed by using field emission scanning electron microscopy (FE-SEM) (HITACHI High Technologies Corporation, S-4800II Japan). The secondary electron images are captured at 15 kV accelerating voltage. As for thermal analysis, thermogravimetric-differential scanning calorimetry (TG-DSC) (NETZSCH STA 449C Germany) is introduced to study the thermal properties of samples. The heating rate is 15 °C min^{-1} from room temperature to 800°C at argon atmosphere. The mass of sample in an 80 uL corundum crucible is about 3 mg. Finally, the X-ray diffraction (XRD) (Bruker, D8 Advance, Germany) analysis is used to figure out the phase in residues after thermal analysis.

2.4 Onset combustion test

To verify and record the characteristics of samples combustion, the heating wire ignition combustion system is designed and made, as shown in Figure 2. The diameter of heating wire is about 0.1 mm. The DC is employed as the power supply. Ignition and combustion processes are recorded by the high-speed camera

(FASTCAM SA-Z Japan) with shutter speed at 50 us per picture. In each ignition and combustion test, the mass weight of sample is about 10 mg (±1 mg) directly touching with the heating wire. Then, the current value on the heating wire increases slowly and gradually. At the moment of ignition, the corresponding current value is recorded, which is set as ignition energy threshold, and in the meanwhile the shutter of high-speed camera is also pressed. A time period of 200 ms before the shutter time can be also recorded which ensures that we can fully document the process from the ignition moment to its extinction. In order to protect the camera from the burning sparks, a transparent tempered glass is placed between the sample and camera.

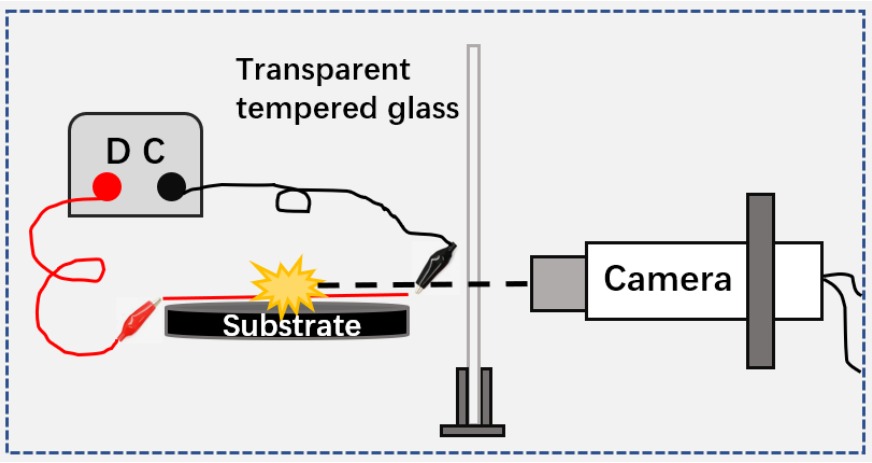

Figure 2 The diagram of onset combustion test

3. Results and Discussion

3.1 SEM analysis

Figure 3 represents the SEM images of Al/MnO_2 and Al/MnO_2/ terpolymer nanothermite samples. Figure 3(a) is the Al/MnO_2nanothermite without the addition of terpolymer. There are two main structures, nanoparticles and nanorods. The nanoparticles represent the fuel, Al NPs, while the nanorods are the oxidizer, MnO_2NRs. The diameter of Al NPs is in the range of 50 nm ˜ 100 nm. The rods length is about several micrometers and the diameter of the rods is merely about 20 nm˜ 50 nm. The Al NPs can directly contact the oxidizer. Besides, the agglomeration phenomenon is not very clear.

Figure 3(b), (c) and (d) are the Al/MnO_2/terpolymer nanothermite with different contents of P(VDF-ter-HFP-ter-TFE) terpolymer, from 10wt% to 30wt% respectively. In Figure 3(b), with 10wt% terpolymer addition, some terpolymer binder can be found among the nanothermite components. In fact, the existence of terpolymer is not pretty obvious due to its content in nanothermite system is not high. So, a fair amount of fuel still can contact direct oxidizer. When the mass fraction of terpolymer reach 20wt% and 30wt%, the existence of terpolymer can be more easily found in Figure 3(c) and (d). As a kind of binder, terpolymer mainly exist among the components, which can bond the nanothermite components together to improve the integrity of the materials.

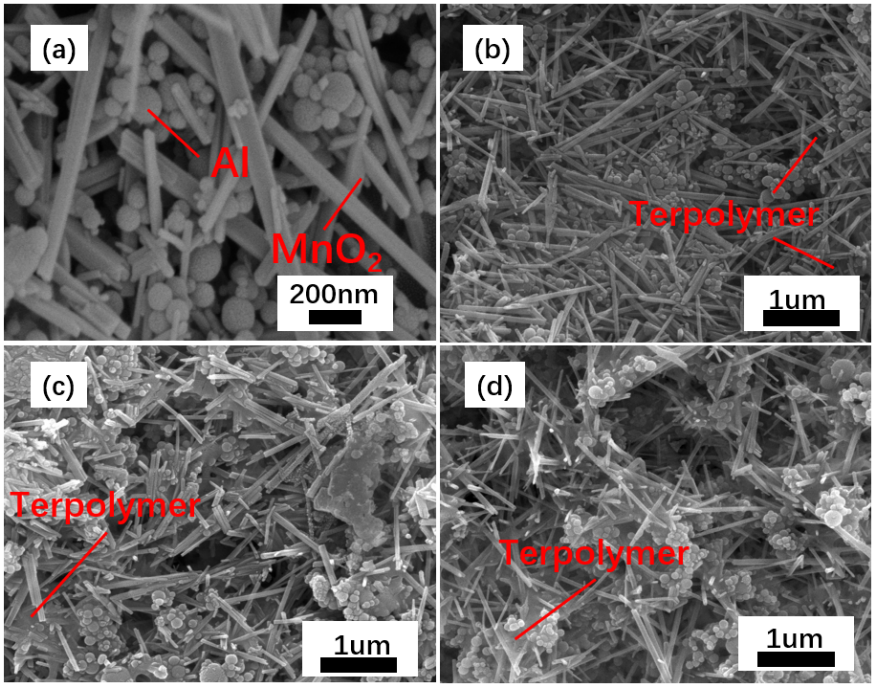

Figure 3 SEM images of nanothermite samples (a) Al/MnO_2 nanothermite, (b) Al/MnO_2/10wt%-terpolymer nanothermite, (c) Al/MnO_2/20wt%-terpolymer nanothermite, (d) Al/MnO_2/30wt%-terpolymer nanothermite

3.2 Simultaneous thermal analysis

We carried out TG-DSC simultaneous thermal analysis tests for Al/MnO_2 and Al/MnO_2/terpolymer nanothermite samples, as shown in Figure 3. The red curves mean the DSC curves while the black curves represent the TG curves within the temperature range from 100°C to 800 °C.

Figure 4(a) illustrates that the TG-DSC results of Al/MnO_2 nanothermite samples. Below 350°C, the total mass continuously loses with the rise of temperature, but there is no obvious endothermic or exothermic DSC signal, which caused by the evaporation of residual solvents, such as free and structural water, ethyl alcohol[28]. The mass is reduced by about 3.0%. Then, in the range of 500 °C ˜600 °C, the main exothermic DSC signal appears, indicating that the thermite exothermic reaction between Al NPs and MnO_2 NRs occurs. At the same time, no obvious mass changes from TG curve at such temperature range. During thermite reaction, the O element transfers from oxidizer, MnO_2NRs, to Al NPs. Thus, no mass change happens. The peak temperature of thermite reaction of Al/MnO_2 nanothermite sample is about 554 °C with the 1070 Jg^{-1} heat release.

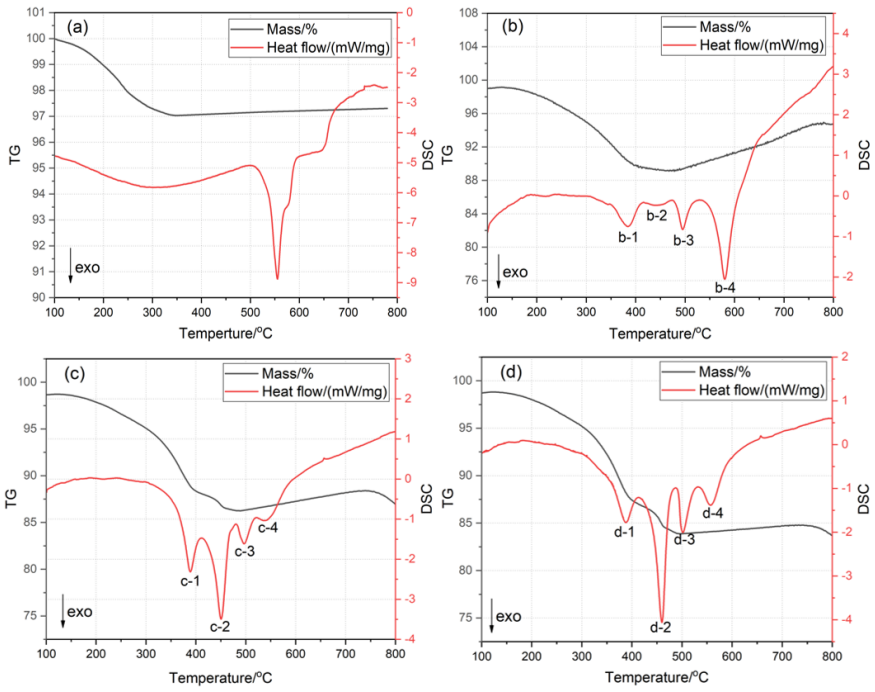

Figure 4 TG-DSC results nanothermite samples (a) Al/MnO_2 nanothermite, (b) Al/MnO_2/10wt%-terpolymer nanothermite, (c) Al/MnO_2/20wt%-terpolymer nanothermite, (d) Al/MnO_2/30wt%-terpolymer nanothermite

Figure 4(b) shows the TG-DSC results of Al/MnO_2/10wt%-P(VDF-ter-HFP-ter-TFE) terpolymer nanothermite sample. At about 472 °C, the minimum of total mass appears, about 89.1%. Considering the evaporation of solvent, more than 80% of terpolymer decomposes to the gaseous products, leading to mass loss. However, D'Orazio and his co-authors [29] have reported the thermal decomposition property of P(VDF-ter-HFP-ter-TFE) terpolymer, and the results shows that all of terpolymer will convert the gaseous products before 500°C. Meanwhile, combined with previous reports [24,30], a few parts of terpolymer react with nanothermite components directly, which can explain those exothermic DSC signals (signal b-1, b-2 and b-3), implying reactions among Al NPs, MnO_2 NRs, terpolymer degradation products and/or the terpolymer matrix. Then, as the temperature increases gradually, the exothermic DSC signal (b-4) occurs, indicating the thermite reaction between remaining Al NPs and MnO_2 NRs, similar to the exothermic signal in Figure 4(a). By contrast, the peak temperature point (b-4) is delayed by 26 °C since some sections of thermite components react with P(VDF-ter-HFP-ter-TFE) terpolymer before.

Next, the content of P(VDF-ter-HFP-ter-TFE) terpolymer reaches 20wt% in Figure 4(c). At about 483 °C, the minimum of total mass appears, about 86.2%, implying that there is 13.8% mass loss. Similarly, it is caused by evaporation of solvent and thermal decomposition of terpolymer. It is inferred that near 50% of terpolymer directly react with the Al NPs and MnO_2 NRs rather than decomposition with gaseous products release, leading to the three exothermic DSC signals (c-1, c-2 and c-3) accordingly[24, 29,30]. Comparing to Figure 4(b), those three exothermic DSC signals (c-1, c-2 and c-3) are bigger and more obvious, especially signal c-2. However, the more proportion of terpolymer reacts with nanothermite components, the less amount of nanothermite components remains for thermite reaction, which results in the corresponding smaller exothermic DSC signal (c-4) for thermite reaction with less heat release.

Finally, the formulation with 30wt% P(VDF-ter-HFP-ter-TFE) terpolymer content is shown in Figure 4(d). At about 491 °C, the minimum of total mass appears, about 83.9%. Same to above reason for mass loss, after estimating, more than 50% of terpolymer directly react with Al NPs and/or MnO_2 NRs, which leads

to the big exothermic DSC signal (d-2). Similarly, much proportion terpolymer reaction with nanothermite components will affect the further thermite reaction and the corresponding exothermic DSC signal (d-4).

Besides, from Figure 4(b), (c) and (d), it can be found that not only the terpolymer itself will influence the thermal reaction process of Al/MnO_2 nanothermite system, but the mass fraction of P(VDF-ter-HFP-ter-TFE) terpolymer also affect the thermal properties and processes. Specifically, from above TG-DSC results, as the content of terpolymer is no more than 10wt%, the main exothermic reaction is still thermite reaction between Al NPs and MnO_2 NRs. In contrast, if the mass fraction of terpolymer is more than 20wt%, the thermite reaction will be greatly decreased and the main exothermic signal will be replaced by the reaction between terpolymer and nanothermite components.

3.3 Residues XRD analysis

From TG-DSC results, it can be clearly found that the addition and content of P(VDF-ter-HFP-ter-TFE) terpolymer can significantly change the thermal processes with the rise of temperature. To further understand the reaction products from different nanothermite samples, we collected the residues in crucible after TG-DSC tests, and used XRD analysis to study the phase of residues, as shown in Figure 5.

Without the addition of terpolymer, the reaction products are mainly Mn_3O_4, MnO and Al_2O_3 caused by thermite reaction between Al NPs and MnO_2 NRs (green curve in Figure 5, AMT-0-residues). Then, the blue curve presents the XRD results of Al/MnO_2/10wt%-terpolymer nanothermite reaction products. The reaction products have mainly changed to galaxite ($MnAl_2O_4$) with some sections of MnO and aluminum manganese (Al_2Mn_3). The red and black curves show the residues of Al/MnO_2/20wt%-terpolymer and Al/MnO_2/30wt%-terpolymer nanothermite samples, respectively, and their reaction products are almost same, containing Al_2O_3, manganese carbide (Mn_7C_3), Al_2Mn_3, MnO, AlF_3, C and remaining Al, which are greatly different from Al/MnO_2/10wt%-terpolymer nanothermite sample as well as Al/MnO_2 nanothermite sample. We guess that the different content of P(VDF-ter-HFP-ter-TFE) terpolymer influences the detailed thermal processes during the TG-DSC tests, and then the different thermal processes lead to the different reaction products finally.

The different content of terpolymer can distinctly change the reaction products. More than 80% terpolymer decompose before the thermite reaction. Namely, few terpolymer and/or terpolymer degradation products involves into thermite reaction. So, the phases of reaction products are mainly $MnAl_2O_4$, MnO and Al_2Mn_3 rather than AlF_3. In contrast, when the content of terpolymer increase, more and more terpolymer react with components, leading to the AlF_3occurrence from residues analysis.

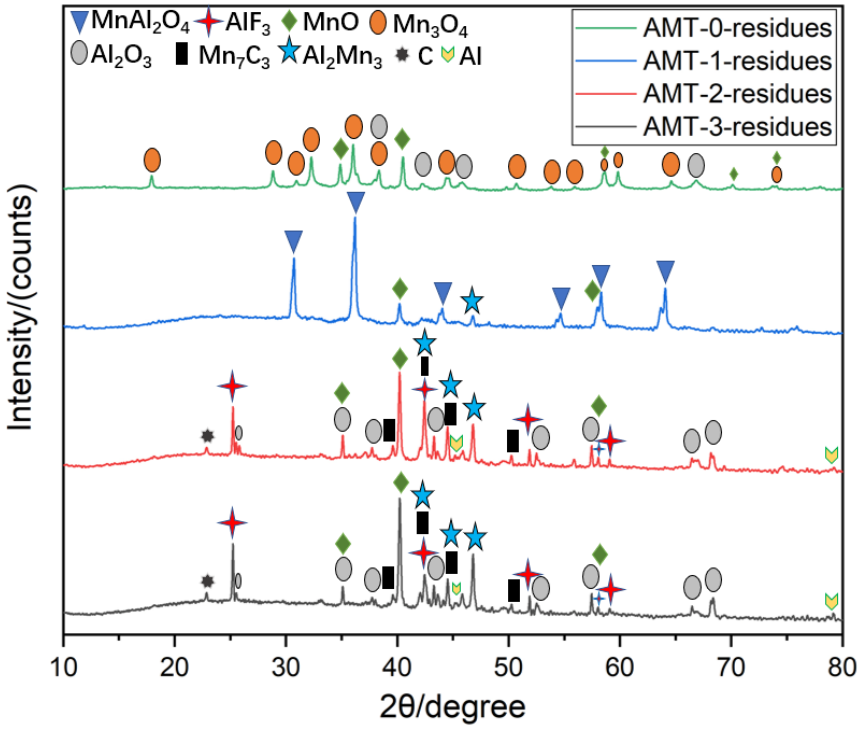

Figure 5 XRD results of residues after TG-DSC tests

3.4 Ignition and combustion

Ignition and combustion performance represent the practical characteristics for energetic materials future application. In this work, we carried out the ignition and combustion by using fast heating wire test as well as high-speed camera. The detailed ignition and combustion performance for each sample is shown in Figure 6. The first picture of a firelight is defined as the beginning time, set as 0 us. The DC power supplier is selected, and the current value for ignition moment is recorded as the ignition energy threshold.

In Figure 6(a), when the current rise to 1.192 A, the Al/MnO_2 nanothermite sample without any additive successfully ignites. The speed of flame grow is very rapid, and at about 350 us, the size of flame reaches the maximum. Then, the flame fades away gradually with clear flying sparks (Supplementary movie 1).

In Figure 6(b), the sample with 10wt%- P(VDF-ter-HFP-ter-TFE) terpolymer additive ignites at about 1.137A current value. The speed of flame growth is still relatively fast, and at about 1 ms, the size of flame reaches the maximum. However, comparing to the Al/MnO_2 nanothermite sample in Figure 6(a), the speed of flame grow and the size of maximum flame are decreased clearly. The addition of terpolymer can help reduce the number of flying sparks to concentrate the flame. Besides, the duration of combustion is longer than that of Al/MnO_2 nanothermite sample (Supplementary movie 2).

Furthermore, when the contents of terpolymer reach 20wt% and 30wt%, the current value at ignition moment are 1.083A and 1.075A, respectively. As for Al/MnO_2/20wt%-terpolymer sample, in Figure 6(c), (Supplementary movie 3) the flame grows pretty slow, and the maximum flame appears at about 7 ms. After the maximum flame moment, the flame seems not to fade away gradually but further forms a certain burning flame shape, which might be caused by the unevenly distributed terpolymer, leading to the ignition delay phenomenon [31-32]. Such phenomenon is also found in the last sample, in Figure 6(d) (Supplementary movie 4). After the maximum flame moment at about 8 ms ˜9 ms, a small but clear bulge appears at the top of flame.

When the contents of terpolymer are below or equal to 10wt%, the phenomenon of ignition delay is not obvious, and the shapes of flame are mainly concentrated sphere. In contrast, once the terpolymer content is over 20wt%, the ignition delay phenomenon and different shapes of flame can be captured. Besides, the addition of P(VDF-ter-HFP-ter-TFE) terpolymer can reduce the ignition energy threshold from the current value at ignition moment, but it has a greatly negative influence on flame growth, leading to the long combustion duration time.

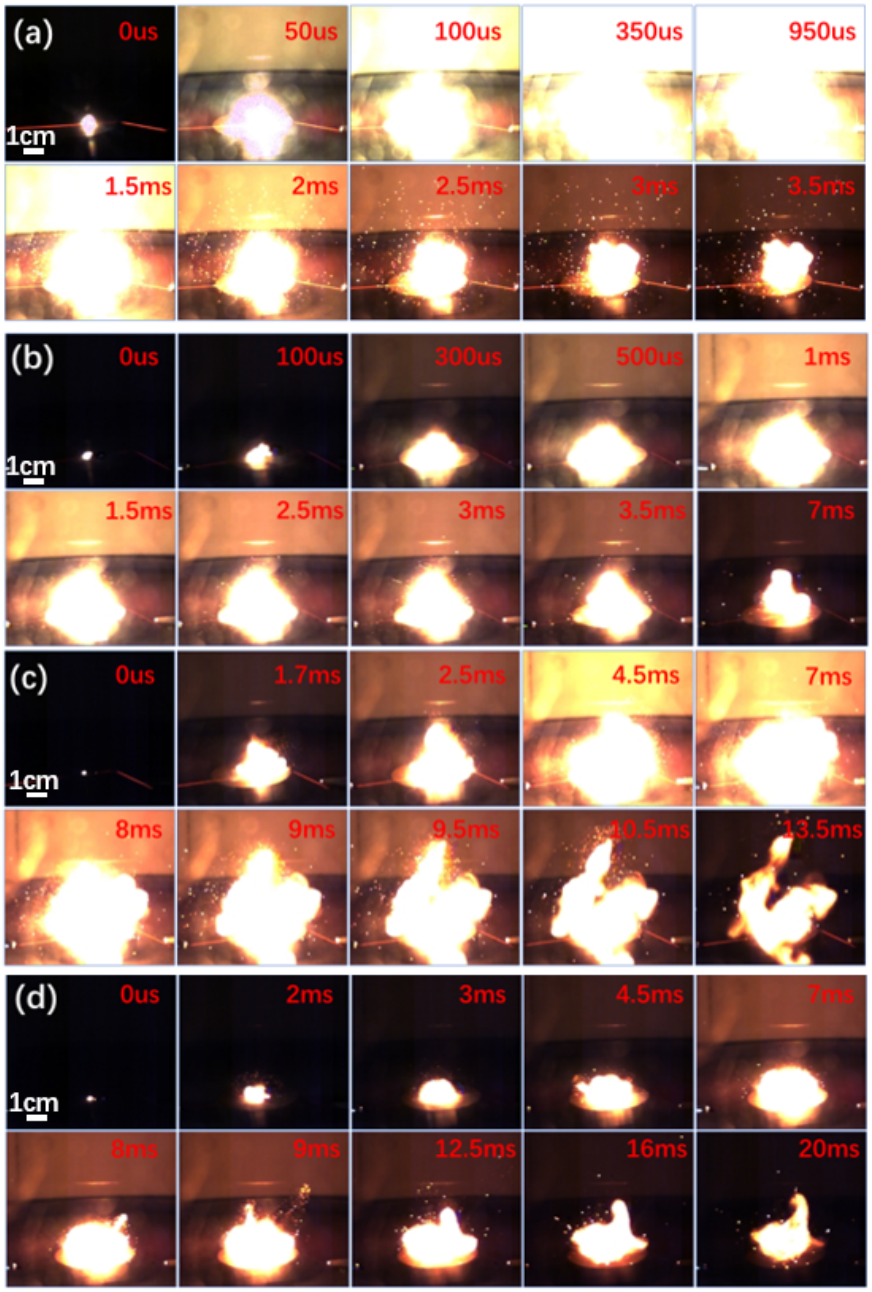

Figure 6 Combustion processes of nanothermite samples (a) Al/MnO_2 nanothermite (Supplementary movie 1), (b) Al/MnO_2/10wt%-terpolymer nanothermite(Supplementary movie 2), (c) Al/MnO_2/20wt%-terpolymer nanothermite (Supplementary movie 3), (d) Al/MnO_2/30wt%-terpolymer nanothermite (Sup-

plementary movie 4)

To further understand the difference of ignition and combustion phenomenon, the potential reasons are analyzed and discussed combined with above morphology, thermal process and residues analysis, as shown in Figure 7. The red arrow presents the direction of flame growth and spread, and its length and width collectively mean the speed of flame growth and spread. From the above results of TG-DSC test, the thermite reaction occurs before the melting point of Al NPs, implying that thermite reaction belongs to solid-phase reaction.

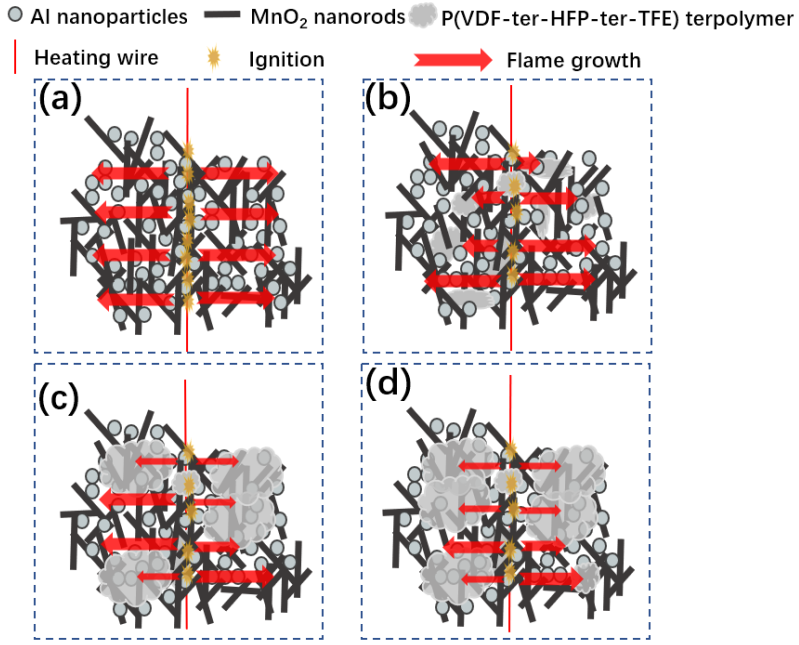

Figure 7 The diagram of different combustion phenomenon, (a) Al/MnO_2 nanothermite, (b) Al/MnO_2/10wt%-terpolymer nanothermite, (c) Al/MnO_2/20wt%-terpolymer nanothermite (d) Al/MnO_2/30wt%-terpolymer nanothermite

As for Al/MnO_2nanothermite (Figure 7(a)), without any addition of terpolymer, the ignition point should be near the heating wire and between the Al NPs and MnO_2 NRs, and then theoretically the flame travels equally fast in each direction.

In Figure 7(b), the 10wt% content of P(VDF-ter-HFP-ter-TFE) terpolymer exists in the gaps among components, decreasing the heat spread and direct contact of nanothermite components. It can be the reason for the delay of flame growth. But the content of terpolymer is not high, so the negative effect on flame growth is not terrible, either. Each coin has two sides. Based on ignition test, the addition of terpolymer can reduce the ignition energy threshold from the current value at ignition moment. The terpolymer is very sensitive to the temperature increment. On one hand, high temperature can lead the process of thermal decomposition with heat release. On the other hand, the decomposition of terpolymer can release the fluoride. The fluoride can directly react with nanothermite components at early stage. Besides, since fluorine is the most electronegative element, it can deal with the alumina shell covered on the Al NPs, leading to the increasing active aluminum directly react with oxidizer.

Figure 7(c) and (d) shows the combustion diagram of Al/MnO_2/20wt%-terpolymer and Al/MnO_2/30wt%-terpolymer nanothermite, respectively. Comparatively, the negative effect on flame growth become increasing great with the increasing content of terpolymer. Terpolymers even totally cover the nanothermite components

in some parts, which leads to the clear ignition delay phenomenon. At the same time, much more heat will release at an early stage due to the more content of terpolymer decomposition as well as reaction with components from TG-DSC results, resulting in a lower ignition energy threshold accordingly.

4. Conclusion

In this paper, the investigation of P(VDF-ter-HFP-ter-TFE) terpolymer additive on Al/MnO_2nanothermite system was presented. The terpolymer can stick nanothermite components together to enhance the integrality of materials. The thermal properties can be significantly influenced by the contents of P(VDF-ter-HFP-ter-TFE) terpolymer. Without any terpolymer additive, thermite reaction between Al and MnO_2 occurred at about 554 °C. For 10wt% mass fraction of terpolymer, three exothermic signals appeared before the main thermite reaction, indicating the thermal reactions among Al nanoparticles, MnO_2 nanorods, terpolymer degradation products and/or the terpolymer matrix. However, those three thermal reactions became the main exothermic reaction instead of thermite reaction when the content of terpolymer was over 20wt%, and the residues analysis verified the difference. The main reaction products of Al/MnO_2nanothermite were Mn_3O_4, MnO and Al_2O_3. For Al/MnO_2/10wt%- terpolymer, the residues were $MnAl_2O_3$ and Al_2Mn_3. When the content of terpolymer was more than 20wt%, such Mn_7C_3 and AlF_3 were found in the residues. The ignition and combustion processes were also different accordingly. The terpolymer could reduce the ignition energy threshold but also decrease the speed of flame growth. The terpolymer could hinder the direct contact of nanothermite components and influence the flame spread. This work revealed the thermal and combustion performance of Al/MnO_2/ P(VDF-ter-HFP-ter-TFE) terpolymer nanothermites, which could provide a reference for application of fluoroelastomer in energetic materials.

Conflicts of interest

The authors declare that there is no conflict of interest regarding the publication of this paper.

Acknowledgements

This work was supported by China Scholarship Council (No. 201903170086), the Natural Science Foundation of Shannxi Province, China (Grant No. 2020JC-50) and School of Mechanical and Aerospace Engineering, Nanyang Technological University (NTU).

References

[1] N.H. Yen, L.Y. Wang. Reactive metals in explosives. Propell. Explos. Pyrot. 37(2012) 143-155. https://doi.org/10.1002/prep.200900050.

[2] C. Rossi, C. Zhang, K. Esteve, D. Alphonse, P. Tailhades, P. Vahlas. Nanoenergetic materials for MEMS: a review. J. Microelectromech. S. 16(2007) 919-931. https://doi.org/10.1109/JMEMS.2007.893519.

[3] L.H. Shen, G.P. Li, Y.J. Luo, K. Gao and Z. Ge. Preparation and characterization of Al/B/Fe_2O_3 nanothermites. Sci. China. Chem. 57(2014) 797-802. https://doi. org/10.1007/s11426-013-5050-2.

[4] Q.H. Wang, S.B. Yang, H.B. Bao, Q.Y. Wang, X.M. Li, W.J. Yang. Self-assembled core-shell structured Si@CuO energetic materials for enhanced exothermic performance. Vacuum. 169(2019) 108881. https://doi.org/10.1016/j.vacuum. 2019.108881

[5] Q.H. Wang, Y.C. Ma, Y.L. Wang, H.B. Bao, A.Q. Li, P. Xu, X.M. Li and W.J. Yang. Facile fabrication of highly exothermic CuO@Al nanothermites via self-assembly approach. Nanotechnology. 31(2020) 055601. https://doi.org/10.1088/1361-6528/ab4ed0.

[6] X. L. Hu, X. Liao, L. Q. Xiao, X. X. Jian, W. L. Zhou. High-energy pollen-like porous Fe_2O_3/Al thermite: synthesis and properties. Propell. Explos. Pyrot. 40(2015) 867-872. https://doi.org/10.1002/prep.201500046.

[7] J. P. Zhang, Y. Y. Zhang, H. Li, J. X. Gao, X. L. Cheng. Molecualr dynamics investigation of thermite reaction behavior of nanostructured Al/SiO_2 system. Acta. Phys. Sin-Ch Ed. 63(2014) 086401.

https://doi.org/10.7498/aps.63.086401.

[8] J. X. Song, T. Guo, M. Yao, W. Ding, X. N. Zhang, F. L. Bei, J. Tang, J. Y. Huang, Z. S. Yu. Thermal behavior and combustion of Al nanoparticles/MnO_2 nanorods nanothermites with addition of potassium perchlorate. RSC Adv. 9(2019) 41319-41325. https://doi.org/ 10.1039/C9RA08663C.

[9] S. Elbasuney. Novel colloidal nanothermite particles (MnO_2/Al) for advanced highly energetic system. J. Inorg. Organomet. P. 28(2018) 1793-1800. https://doi.org/ 10.1007/s10904-018-0823-x.

[10] C. P. Yu, W. C. Zhang, R. Q. Shen, X. Xu, J. Cheng, J. H. Ye, Z. C. Qin, Y. M. Chao. 3D ordered macroporous NiO/Al nanothermite film with significantly improved higher heat output, lower ignition temperature and less gas production. Mater. Design. 110(2016) 304-310. https://doi.org/10.1016/j.matdes.2016.08.002.

[11] J.X. Song, T. Guo, M. Yao, J.L. Chen, W. Ding, F.L. Bei, Y. Mao, Z.S. Yu, J.Y. Huang, X.N. Zhang, Q Yin, S Wang. A comparative study of thermal kinetics and combustion performance of Al/CuO, Al/Fe_2O_3 and Al/MnO_2nanothermites. Vacuum. 176(2020) 109339. https://doi.org/10.1016/j.vacuum.2020.109339.

[12] S.K. Valluri, M. Schoenitz, E. Dreizin. Fluorine-containing oxidizers for metal fuels in energetic formulations. Def. Technol. 15(2019) 1-22. https://doi.org/ 10.1016/j.dt.2018.06.001.

[13] K. Jahnisch, M. Baerns, V. Hessel, W. Ehrfeld, V. Haverkamp, H. Lowe, Ch. Wile, A. Guber. Direct fluorination of toluene using elemental fluorine in gas/liquid microreactors. J. Fluorine. Chem. 105(2000) 117-128. https://doi.org/ 10.1016/S0022-1139(00)00300-6.

[14] X. Zhou. D. G. Xu, J. Lu, K. L. Zhang. CuO/Mg/fluorocarbon sandwich-structure superhydrophobic nanoenergetic composite with anti-humidity property. Chem. Eng. J. 266(2015) 163-170. https://doi.org/10.1016/j.cej.2014.12.087.

[15] X. Zhou, D. G. Xu, G. C. Yang, Q. B. Zhang, J. P. Shen, J. Lu, K. L. Zhang. Highly exothermic and superhydrophobic Mg/fluorocarbon core/shell nanoenergetic arrays. ACS Appl. Mater. Inter. 6(2014) 10497-10505. https://doi.org/ 10.1021/am502078e

[16] K. Meeks, M. L. Pantoya, C. Apblett. Deposition and characterization of energetic thin films. Combust. Flame. 161(2014) 1117-1124. https://doi.org/10.1016 /j.combustflame.2013.10.027

[17] X. Zhu, S. S. Feng, S. F. Zhao, C. Xu, M. Hu, Z. X. Zhong, W. H. Xing. Perfluorinated superhydrophobic and oleophobic SiO_2@PTFE nanofiber membrane with hierarchical nanostructures for oily fume purification. J. Membrane. Sci. 594(2020) 117473. https://doi.org/10.1016/j.memsci.2019.117473.

[18] J. Khedkar, I. Negulescu, E. I. Meletis. Sliding wear behavior of PTFE composites. Wear. 252(2002) 361-369. https://doi.org/10.1016/S0043-1648(01)00859-6.

[19] D. H. Li, M. Y. Liao. Dehydrofluorination mechanism, structure and thermal stability of pure fluoroelastomer (poly(VDF-ter-HFP-ter-TFE) terpolymer) in alkaline environment. J. Fluorine. Chem. 201(2017) 55-67. https://doi.org/ 10.1016/j.jfluchem.2017.08.002

[20] W. J. Ye, T. Wang, Y. H. Yu. Research progress of fluoropolymer-matrix energetic reactive materials. Aerospace Materials & Technology. 42(2012) 19-23.

[21] L. L. Ding, J. Y. Zhou, W. H. Tang, X. W. Ran, Y. X. Hu. Impact energy release characteristics of PTFE/Al/CuO reactive materials measured by a new energy release testing device. Polymers. 11(2019) 149. https://doi.org/10.3390/polym11010149

[22] J. Y. Zhou, L. L. Ding, W. H. Tang, X. W. Ren. Experimental study of mechanical properties and impact-induced reaction characteristics of PTFE/Al/CuO reactive materials. Materials. 13(2020) 66. https://doi.org/10.3390/ma13010066.

[23] J. X. Wu, Q. Liu, B. Feng, S. Z. Wu, S. Zhang, Z. R. Gao, Q. Yin, Y. C. Li, L. M. Xiao, J. Y. Huang. A comparative study on the mechanical and reactive behavior of three fluorine-containing thermites. RSC

Adv. 10(2020) 5533-5539. https://doi.org/ 10.1039/D0RA00044B.

[24] C. Huang, H. Yang, Y. Li, Y. Cheng. Characterization of aluminum/poly(vinylidene fluoride) by thermogravimetric analysis, differential scanning calorimetry, and mass spectrometry. Anal. Lett. 48(2015) 2011-2021. https://doi.org/10.1080 /00032719.2015.1012675.

[25] H. Hori, H. Tanaka, T. Tsuge, R. Honma, S. Banerjee, B. Ameduri. Decomposition of fluoroelastomer: poly(vinylidene fluoride- ter -hexafluoropropylene - ter- tetrafluoroethylene) terpolymer in subcritical water. Eur. Polym. J. 94(2017) 322-331. https://doi.org/10.1016/j.eurpolymj.2017.05.042.

[26] J.X. Song, X. Fang, T. Guo, F. L. Bei, W. Ding, X. N. Zhang, M. Yao, H. J. Yu. Thermal properties and kinetics of Al/alpha-MnO_2 nanostructure thermite. J. Brazil. Chem. Soc. 29(2018) 404-411. https://doi.org/10.21577/0103-5053.20170154.

[27] N. N. Zhao, C. C. He, J. B. Liu, H. X. Ma, T. An, F. Q. Zhao. Preparation and characterization of superthermite Al/MnO_2 and its compatibilities with the propellant components. Chinese Journal of Explosives and Propellants. 35(2012) 32-36. https://doi.org/10.14077/j.issn.1007-7812.2012.06.018.

[28] W. M. Dose, S. W. Donne. Manganese dioxide structural effects on its thermal decomposition. Mater. Sci. Eng. B. 176(2011) 1169-1177. https://doi.org/10.1016/ j.mseb. 2011.06.007.

[29] L. D'Orazio, G. Gentile, C. Mancarella, E. Martuscelli, V. Massa. Water-dispersed polymers for the conservation and restoration of cultural heritage: a molecular, thermal, structural and mechanical characterization. Polym. Test. 20(2001) 227-240. https://doi.org/10.1016/S0142-9418(00)00027-1.

[30] X. Y. Li, C. Huang, H. T. Yang, Y. C. Li, Y. Cheng. Thermal reaction properties of aluminum/copper (II) oxide/ poly(vinylidene fluoride) nanocomposite. J Therm. Anal. Calorim. 124(2016) 899-907. https://doi.org/10.1007/s10973-015-5194-8.

[31] S. G. Hosseini, A. Sheikhpour, M. H. Keshavarz, S. Tavangar. The effect of metal oxide particle size on the thermal behavior and ignition kinetics of Mg-CuO thermite mixture. Thermochim. Acta. 626(2016) 1-8. https://doi.org/10.1016/ j.tca.2016. 01.005

[32] E. L. Dreizin. Metal-Based Reactive nanomaterials. Prog Energ. Combust. 35(2009) 141–167. https://doi.org/10.1016/j.pecs.2008.09.001.